Astron. Astrophys. 358, 1049–1057 (2000)

ASTRONOMY AND ASTROPHYSICS

The intrinsic structures of circular and elliptical planetary nebulae

J.P. Phillips

Instituto de Astronomia y Meteorologia, Av. Vallarta No. 2602, Col. Arcos Vallarta, C.P. 44130 Guadalajara, Jalisco, Mexico

Received 14 December 1999 / Accepted 23 March 2000

Abstract. Planetary nebula axial ratios have been used to investigate the intrinsic structures of sources having elliptical or circular morphologies, using methods previously applied to elliptical galaxies. The results appear to indicate that most such nebulae have intrinsic axial ratios β in the range $0.92 \rightarrow 0.75$, and that gradients of surface brightness with axial ratio are most consistent with oblate shell structures. It remains possible however, given the uncertainties in the analysis, that many circular or ellipsoidal planetary nebulae also have prolate configurations. Whilst there may be evidence for an evolution of axial ratio with nebular radius, there appears to be little variation with Galactic latitude. This would suggest that nebular asphericities are not, in the main, dependent upon interaction with the interstellar medium, and that the variation of axial ratio with progenitor mass is also quite low.

Key words: ISM: planetary nebulae: general – ISM: structure

1. Introduction

Investigations of the morphologies of planetary nebulae have revealed as many as 17 differing categories of shell structure, ranging from classically circular sources (a quite rare commodity as it turns out) through to bipolar and irregular nebulae (e.g. Kromov & Kohoutek 1968; Greig 1972; Zuckerman & Aller 1986; Schwarz et al. 1993; Manchado, Guerrero & Stanghellini et al. 1996).

The origins of these differing morphologies remains a matter of speculation, although it is possible that bipolar sources derive from progenitors within binary systems (Bond & Livio 1990); where stars are engirded by planetary systems (Sahai et al. 1991); or perhaps through the action of magnetic fields (Pascoli 1987). Alternatively, it seems possible that elliptical shells may arise through the coupling of low mass companions (large planets or brown dwarfs) with superwind outflows (Soker 1992), or through the effects of stellar rotation, together with shocks and/or photospheric dust condensation (Asida & Tuchman 1995; Dorfi & Hofner 1996). An attempt to explain global properties in terms of ejection mechanisms has been outlined by Balick (1987).

Send offprint requests to: J.P. Phillips

Before being able to assess the viability of such mechanisms, however, it is clearly desirable to know something of the intrinsic structures of these sources; a problem which is, as it turns out, far from easy to resolve. Although it is likely that bipolar sources do indeed possess intrinsically bipolar structures, collimated by circum-nebular disks, and that most elliptical/circular structures derive from spheroidal nebulae, it is far from easy to establish whether this is unambiguously the case for all such nebulae. One method for determining PN structures is, for instance, to combine kinematic and morphological data to arrive at self-consistent solutions (Weedman (1968) and Wilson (1958) represent two early and more general analyses of this type, although a multiplicity of individual source studies have also been undertaken (see for instance the discussion of NGC 6720 below)). Such methods are however far from fool-proof, and have been applied to only a limited proportion of sources. These analyses are also dependent upon model assumptions; they often presume for instance that the velocity of expansion is proportional to nebular radius. Such assumptions may be applicable to certain nebulae, but less relevant for the generality of sources.

A case in point - and one which emphasises the uncertainties in such analyses, and the way that our understanding of shell structures may evolve with time - is that of the well-known ring nebula NGC 6720. Its morphology may at first sight appear to imply an intrinsically spheroidal shell structure, and this was indeed suggested by Gurzadyan (1970), Atherton et al. (1978), Curtis (1918) and many others. More recent investigations however have suggested that the bright optical ring is disk-like (Lame & Pogge 1994), and that this disk is collimating a bipolar flow oriented along the line of sight (Bryce et al. 1994). It is interesting however to note that certain of the evidence used to deduce the toroidal structure (high ring/centre intensity ratios in low excitation lines) is inconsistent with the variation in intensities and kinematics for higher excitation transitions (Atherton et al. 1978; Kupferman 1983), and may be misconceived (Phillips & Reay 1980). Unresolved filaments and sheets may lead to precisely similar outcomes. It is therefore possible that our understanding of this source will be found to have followed a closed loop, and that the source is as it first appeared (a spheroidal nebula).

Placing the doubts concerning this particular source to one side, it seems likely that many bipolar nebulae are indeed being viewed pole-on, and that certain ellipsoidal or circular nebulae may represent disks. Given however that most nebulae are circular or elliptical (2/3 of sources in the IAC Morphological Catalog are so (Manchado et al. 1996)), and that the proportion of highly elongated sources is proportionately low, it seems that most PN are more likely to be spheroidal (see also our later comments).

This, in turn, introduces another area of uncertainty. Whilst many models of PN formation would favour oblate shell structures (certainly those postulating stellar rotation or planetary interaction as the dominant shaping mechanisms), others favour explanations in terms of prolate shocks and shell structures (e.g. Livio et al. 1996; Balick et al. 1987). There is kinematical evidence to favour both of these options, and it is just as possible (given the observed morphologies) that PN shells are intrinsically oblate or prolate. It might even be possible that certain ellipsoidal shells arise from tilted cylindrical shells (see for instance Volk & Leahy (1993)) - although such cases might alternatively be explained in terms of evolved prolate structures, in which the major axis limits of the shells are faint, or have been disrupted and removed by interior nebular winds.

This ambiguity (whether shells are prolate or oblate) engenders a sense of deja vu, since it is precisely such uncertainties that used to inform studies of elliptical galaxies. In fact, and as we now know, many elliptical galaxies may not be axi-symmetric so much as triaxial (Fasano & Vio 1991; Merritt 1992). Nevertheless, the methods employed to investigate the oblate/prolate ambiguity in galaxies may also be applied to PN.

There are at least three main ways in which this may be undertaken. In the first of these, one may "deconvolve" the observed distribution of axial ratios by assuming random orientations of the PN to the line of sight; a procedure which has been outlined by Mihalas & Binney (1981) for galaxies, and applied with varying degrees of sophistication by Sandage et al. (1970), Ryden (1996), and Tremblay & Merritt (1995). By bringing an armoury of statistical weapons to bear upon this question, such authors have claimed to show that the intrinsic distribution of ellipticities would be non-physical were galaxies spheroidal and axi-symmetric (i.e. prolate or oblate). In reality, however, we are inclined to believe that this procedure is of itself unsatisfactory (at least, it would be so where it is applied to PN); the range of data which determines whether sources are, or are not axi-symmetric is quite small, and represents but a small proportion of the total data set, whilst errors in observed axial ratios may be appreciable (around 7% or so in the mean; see Sect. 2).

We therefore favour combining this procedure with a second method outlined by Marchart & Olsen (1979), whereby observational trends of surface brightness with axial ratio are used to distinguish between oblate and prolate model solutions.

A further procedure, based upon an algorithm published by Lucy (1974), attempts to fit solutions for the distribution of intrinsic ellipticities by means of an iterative procedure; a method which has been applied by Binney & de Vaucouleurs (1981), Fasano & Vio (1991) and others. This will not however be employed in the present analysis.

In the following, therefore, we shall be intent to determine how far such methods, so successfully applied to galaxies, may also be used to investigate the structures of planetary nebulae. We shall show that the range of intrinsic axial ratios β is modest, and that shells are most likely to be oblate - certainly, such solutions would seem to offer the best fit to observed trends. However, it will also become clear that it is less easy to discriminate between prolate and oblate shells than was the case for galaxies, and that the analysis of PN structures is a significantly more complex undertaking.

Finally, we shall use the data to investigate evolutionary trends in ellipticity, and the possible influences of the ISM and progenitor mass in leading to shell asphericities.

2. Observational data set

2.1. Optical data base

We have assessed axial ratios for some 204 nebulae, based (primarily) upon imaging published by Manchado et al. (1996), Perek & Kohoutek (1967), Schwarz et al. (1992), Bassgen et al. (1999), and upon more than 70 images deriving from the HST (see for instance Hajian 1999). We have selected images which appear well resolved, and derive (where possible) from exposures in Hα or H β; images, that is, which are likely to provide an accurate indicator of structure within the primary ionised mass.

There are various deficiencies in this data, and it is as well to make these clear from the beginning. The first of these is that although the sources selected are usually very much greater in size than the seeing disk (at least, so far as can be assessed from images of neighbouring field stars), it remains possible that certain of the smaller sources may be "rounded" somewhat; that axial ratios in a small proportion of the sources may be greater than is intrinsically the case.

The second problem is that HI images are not available for all of the sources; indeed, the greater proportion of the images used here are based upon broad-band exposures, or upon exposures in other ionic transitions (such as [NII] or [OIII]). Whilst the axial ratios of many of the sources appear invariant with ionic transition, this is not true in all cases; a few sources (and one may cite A78 and NGC 3587 ("The Owl") as typical cases) appear to have slightly differing axial ratios in differing transitions (e.g. Manchado et al. 1996) - a difference which may be enhanced through varying shell intensities and photographic exposure periods.

Measures of independent images for a variety of sources suggests that mean errors in axial ratio are of order $\Delta\alpha \sim 0.07$.

Finally, it should be emphasised that unlike the case of elliptical galaxies, for which there are a cornucopia of contour maps, there are relatively few such maps available for PN; one must rely on non-systematic data bases of CCD and photographic images (although see also our later remarks concerning radio maps). Not only that, but it is clear that whilst elliptical galaxies display a great structural uniformity (i.e. they display sim-

ilar trends of surface brightness with radius), this is again not the case with elliptical or circular PN. The latter sources may be sharp-edged, or fade away gradually with increasing radius, they may be "filled" structures or ring-like. There is, in brief, a greater variation in PN surface brightness characteristics than is observed in galaxies.

As noted in Sect. 1, certain of the sources may actually represent disks rather than spheroids; and although the proportion of disks is probably low (for reasons also given in Sect. 1) it is clear that they may bias the analysis to be presented below. Given for instance that the projected axial ratios of the disks vary as cos(θ), it is easy to show that such sources would lead to a much larger proportion of sources at low values of α (α< 0.5 say) than would be expected for spheroids.

Finally, we note that certain nebulae may contain multiple shells, and it is pertinent to ask which of these envelopes it is appropriate to measure. Examples of this phenomenon have been noted by Chu et al. (1987), Jewitt et al. (1986), Hajian et al. (1997), and Balick et al. (1992), wherein it would appear that many PN are enveloped by faint (and more-or-less circularly symmetric) shells.

These outer shells are most likely to arise through prior phases of mass-loss along the red giant branch, or multiple phases of ejection along the AGB. They have been observed in only a small proportion of sources, and are not included in the present analysis.

A further type of double envelope structure has been noted in sources such as NGC 7009, NGC 2392, NGC 3242 and so forth. The secondary envelopes are in this case much brighter than the halos cited above, although they are again fainter than the primary (interior) shells. It seems likely that they arise through the recession of ionisation fronts at a turn-around phase in stellar evolution; a period during which the central-star hydrogen-burning layers become exhausted, and ionising fluxes decrease (Phillips 2000). We have, for these cases, included axial ratios for both of the shells, although they again represent but a small fraction of the total nebular data base.

Finally, it should be emphasised that given the image selection techniques described above, then there will be a bias against intrinsically smaller nebulae (which are too compact to resolve) and larger sources (which are too faint to adequately image or detect); indeed, we shall note that most of the present sample lies within a radial range Δ log(R/pc) $\sim$ 2. Where there is any evolution in ellipticities (viz. the discussion in Sect. 5), then this may impose a greater uniformity upon axial ratios than is in reality the case.

2.2. Radio data base

In addition to the optical data cited above, we have sought to incorporate the results of radio mapping by George et al. (1974), Terzian et al. (1974), Kwok (1985), Basart & Daub (1987), Zijlstra et al. (1989), and Phillips & Mampaso (1988); we shall later note that the two sets of data (optical and radio) refer to substantially differing collections of sources; the overlap in the data sets is comparatively small.

The ratios derived from radio mapping are again not entirely free from bias. Thus for instance, although the mapping data base is appreciable, the number of sources observed with low relative beam size is proportionately small. Even in these latter cases (and particularly where beams are non-circular) the beams may be such that deconvolution of the results leads to significant changes in axial ratio. We have therefore been careful to deconvolve all of the results using quoted beams, and by assuming the beams to have Gaussan cross-sections along any particular position angle.

A second problem arises from the limited dynamic ranges of many of the radio maps (i.e. the restricted ranges in surface brightness measured through radio interferometric techniques) compared to equivalent optical imaging. This, in turn, means that such maps pick-out out only the brightest parts of a shell, and may give a misleading impression of the overall shell structures. An example of this is NGC 7293, where optical imaging shows the presence of an oblong (and somewhat disrupted) shell which is significantly fainter towards the major axis limits. The geometric configuration of this shell would suggest ratios $\alpha \cong$ 0.77. In the radio maps, on the other hand, only the brighter more complex structure is fully revealed, implying axial ratios which are significantly greater ($\cong$ 0.89).

Fortunately, a comparison of optical and radio measures of α (see below) suggests that such biases are relatively infrequent.

The limited dynamical range of the radio maps may also make it difficult to discriminate between spherical and other nebular structures. In the cases of bipolar nebulae, for instance, it is clear that we are in many cases detecting only the bright (toroidal?) nuclei, leaving the tell-tale outer structures to be missed altogether. Fortunately however, such nebulae can usually be identified using optical imaging, and appropriately weeded-out.

Finally, it is worthwhile pointing out that as for the optical results mentioned above, the radio mapping is open to quite severe source selection effects; biases which will require incorporating in our later statistical modelling (see Sect. 4). We have noted above, for instance, that the optical results are biased against sources which are very small or large; and these comments are even more apposite in the case of the radio mapping. Fainter (and larger) Abell-type structures are, for instance, recorded to only low levels of S/N (where they are mapped at all); and indeed, most such nebulae remain still to be measured. Certain smaller nebulae have been resolved through the use of long-baseline interferometry - although even here beam sizes are usually such as to preclude a reliable determination of α.

This limited range in shell radii leads, in turn, to a restriction in the nebular mass range - a constraint which is of great relevance for our later statistical modelling.

In order to investigate the nature of this constraint in more detail, we note first that root mean square (rms) densities appear to decline monotonically with increasing nebular radii, and that the scatter in this trend is low (cf. Fig. 1, where we show the variation in n_e(rms) adapted from Phillips (1998)). It may be noted from Fig. 1 that dlog(n_e(rms))/dlog(R) $\cong$ -1.94. This, in turn, implies that shell masses vary as log(M) $\propto$1.065log(R), and

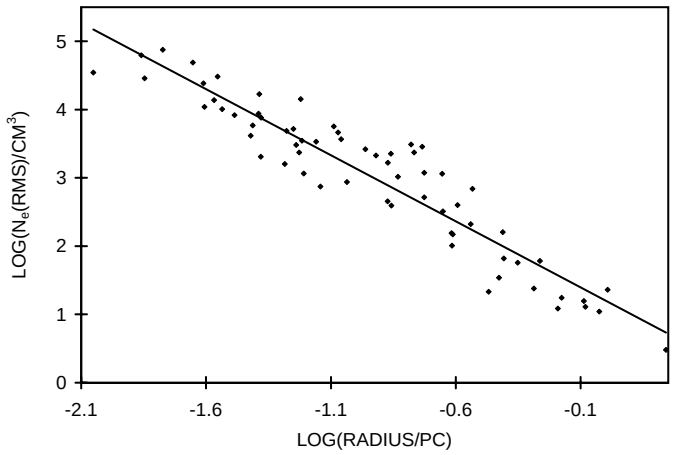

Fig. 1. Variation of rms electron densities for planetary nebulae having model-independent distances. The data is based upon an analysis by Phillips (1998)

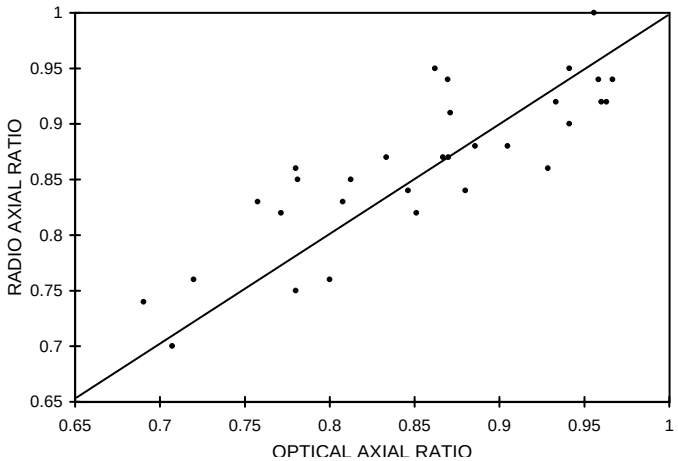

Fig. 3. Comparison of axial ratios for the 31 sources common to both the radio and optical data samples. The solid diagonal line corresponds to a one-to-one relationship

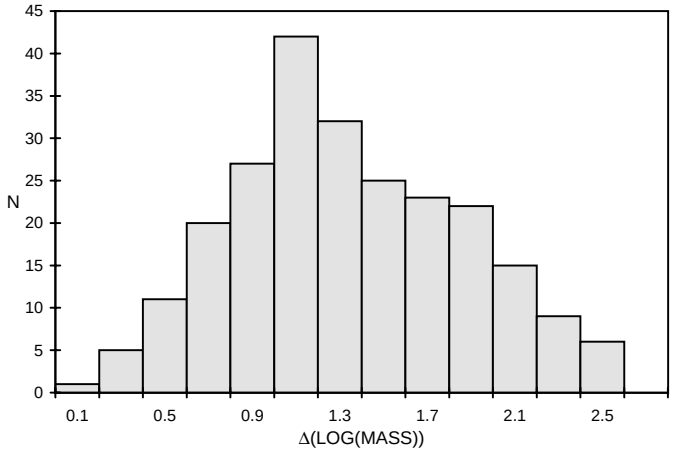

Fig. 2. The distribution of shell masses for the combined optical and radio data sample. It should be noted that the zero point of the data is set arbitrarily at zero

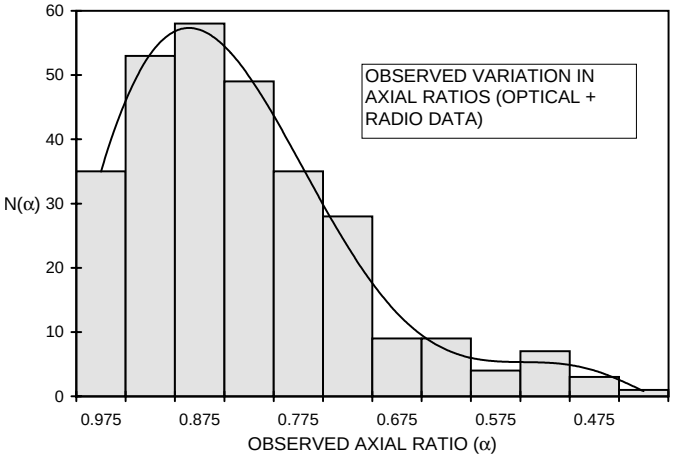

Fig. 4. Histogram of the observed distribution N(α) in axial ratios α, together (solid curve) with a sixth order polynomial least squares fit

such a relation can then be used to evaluate the mass distribution of nebulae in the combined optical and radio sample.

This mass distribution is illustrated in Fig. 2, where we have used statistical distances and angular radii from Zhang (1995) in order to determine R. Note, also, that we are representing here the relative variation in shell mass; the zero point of the mass function is of no relevance for our later modelling.

It is clear, from this, that most sources occupy a regime of masses which is quite narrow, and of order $\Delta\log(M) \sim 1.6$.

Finally, a comparison of the radio and optical axial ratios is illustrated in Fig. 3; where it will be noted that although the overall data base (optical and radio combined) includes some 320 sources, only 31 nebulae are common to both lists (if one excludes NGC 7293 mentioned above). Several conclusions may be drawn from this comparison.

The first is that despite the caveats outlined above, the optical and radio estimates of α appear in reasonable concordance. Second, it would seem that the agreement is sufficiently secure that one may concatenate the two data sets for the purpose of statistical analysis.

Finally, we note that where axial ratios are later compared to radio surface brightnesses, it would seem reasonable to use the combined radio and optical ratios in such an analysis.

It is clear, therefore, that great care should be taken in interpreting these results, although we believe that they are for the most part accurate; certainly the general trends are so. Similarly, we believe that the conclusions which will be reached are trustworthy, although the statistical significance of the results is less than can be achieved for comparable samples of galaxies.

3. Intrinsic distribution of axial ratios

The histogramic distribution in observed axial ratios for circular and elliptical PN is illustrated in Fig. 4, whence it is seen that peak values occur close to $\alpha = 0.89$, and that there is a long tail extending down to $\alpha = 0.43$. We have fitted this distribution with a sixth order least squares polynomial regression curve (solid

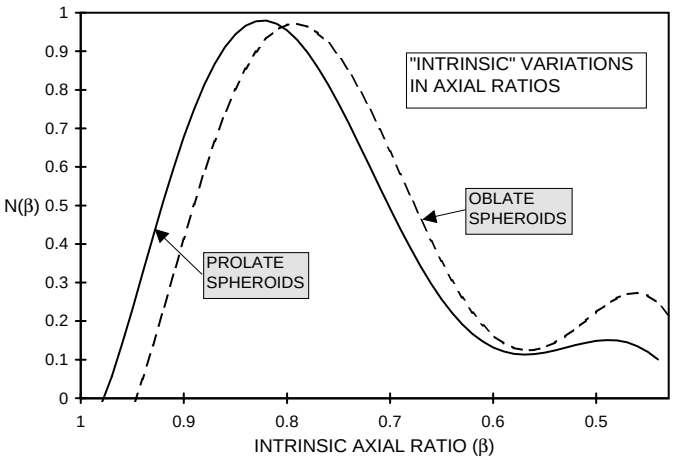

Fig. 5. The distributions of intrinsic axial ratios β predicted where nebulae have oblate or prolate structures. Note that both distributions (prolate and oblate) are similar, and reasonably strongly peaked about β = 0.82. The analysis responsible for these curves is based upon a normalised version of the function N(α) illustrated in Fig. 3

curve), and the normalised version of this curve will be taken to represent the observed function N(α) in our later analyses of intrinsic axial distributions. Small deviations between the least squares fit and histogram are statistically insignificant.

The procedure for determining the intrinsic distribution of axial ratios β for a randomly oriented population of spheroids has been outlined by Mihalas & Binney (1981), who note that

$$N(\alpha) = \alpha^n \int_0^\alpha \frac{N(\beta)\beta^p d\beta}{\sqrt{1-\beta}\sqrt{\alpha^2-\beta^2}}$$

where n = 1 and p = 0 for oblate spheroids, and n = -2, p = 2 for prolate spheroids. The corresponding inverse form of this expression is given by (Tremblay & Merritt 1995)

$$N(\beta) = \frac{4}{\pi}\beta^m\sqrt{1-\beta^2}\frac{d}{d\beta^2}\int_0^\beta \frac{N(\alpha)\alpha^q d\alpha}{\sqrt{\beta^2-\alpha^2}}$$

where m = 1, q = 0 for oblate spheroids, and m = -1, q = 3 for prolate spheroids. It should be noted that β and α are both defined as the ratio of the minor axis to the major axis (respectively a_i and b_i in the case of β, and a_0 and b_0 for α), and that they are therefore both less than unity.

We have used these relations to determine the distribution of sources N(β) illustrated in Fig. 5.

As may be seen, the distribution in axial ratios would be closely similar where sources are oblate or prolate; the oblate spheroids being biased by $\Delta\beta \sim 0.03$ to lower values compared to the prolate solutions. The slight increase in N(β) for β < 0.55 is probably not significant, as is also the case for the negative-going trend where β> 0.95. The tendency for N(β) to be less than zero at high values of β arises because of the functional relation adopted for N(α); a trend which somewhat under-represents sources having α = 1. A very similar negative going trend has also been noted for elliptical galaxies. Whilst Tremblay & Merritt (1995) analyse this negative variation in detail, and attempt to come to far-reaching statistical conclusions, we are inclined to view such analyses as futile - at least where they are applied to PN. Such high axial ratio regimes depend upon far too few data points, and cannot be considered in any way reliable.

A further point to note is that some of the more highly elongated sources may, in particular, have been mis-classified. This problem of mis-classification washes both ways however (i.e. a few sources may be erroneously classified as elliptical, and vice versa), and in any case affects only a small proportion of the sources. Our conclusion is that whilst the distribution of sources having β < 0.55 is unreliable, it is almost certainly qualitatively correct.

Taken as a whole, it is apparent that most circular and elliptical PN possess intrinsic ratios lying between β = 0.6 and 0.95; a conclusion which represents a useful datum in the proceeding analysis.

4. Variation of surface brightness with axial ratio

As has been noted by Marchant & Olsen (1979), the trend of surface brightness I_s with axial ratio α should be quite different depending upon whether galaxies are prolate or oblate; oblate galaxies are expected to yield gradients $dI_s/d\alpha < 0$, whilst gradients for prolate galaxies would be positive. The analysis for planetary nebulae is comparable, although not identical.

Thus, for instance, the observed axial ratio for a spheroidal planetary nebulae will vary as

$$\alpha = (\cos^2\theta + \beta^r \sin^2\theta)^s$$

with respect to the angle θ between the line of sight and axis of nebular symmetry, where r = 2, s = 0.5 for oblate spheroids, and r = -2, s = -0.5 for prolate spheroids. Where the total radio or Balmer line emission is given by F_{TOT}, it then follows that surface brightness is given through $I_s = F_{TOT}/\pi a_0 b_0$.

Given that we shall later compare observed axial ratios with radio surface brightnesses T_b, it is appropriate also to note that F_{TOT} is expected to vary closely as $\propto {n_e}^2 V$, where n_e is the mean electron density and V is the nebular volume. We shall assume that n_e depends upon the harmonic mean nebular radius R_{HM} in a monotonic manner; that is, that $n_e \propto {R_{HM}}^\gamma$ (see discussion in Sect. 2.2); where R_{HM} is given by $(a_i\ {b_i}^2)^{0.33}$ for oblate sources, by $({a_i}^2 b_i)^{0.33}$ for prolate sources, and γ is a constant.

What, in general, might be expected for such a model simulation of surface brightness trends? The first thing to note is that when a nebula is prolate, then I_s would be expected to increase with increasing projected axial ratio α. We have illustrated this tendency in Fig. 6, where we indicate the cases where the axial ratio a_i/b_i = 0.4 is constant and only the angle of inclination varies (solid curves), and where θ = 0, and a_i/b_i varies between 0.4 and 1 (dashed curves). The curves have differing gradients, but the tendencies are identical; $d\log(I_s)/d\alpha$ is in all cases positive. In the case of oblate spheroids, on the other hand, the trends would be precisely the reverse, and we would predict values of $d\log(I_s)/d\alpha$ which are negative.

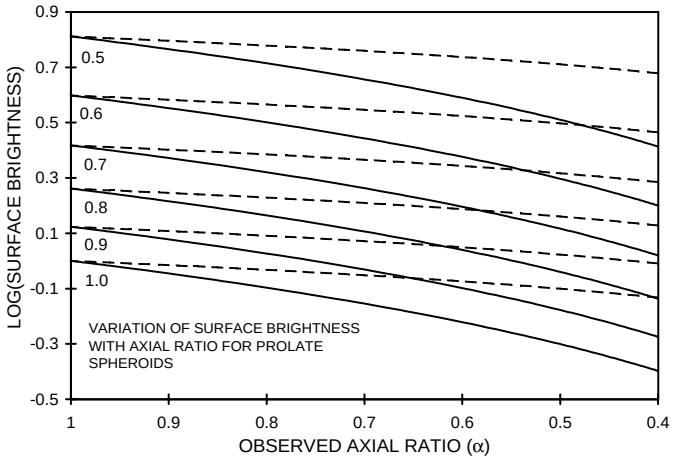

Fig. 6. The variation of surface brightness with axial ratio anticipated for prolate spheroids, given that a) the intrinsic axial ratio (a_i/b_i) = 0.4 is constant, and changes in ellipticity occur through varying angles of inclination θ (solid curves); and b) θ = 0, but (a_i/b_i) is variable (dashed curves). Both of these analyses yield positive gradients $d\log(I_s)/d\alpha$, with individual curves corresponding to differing relative shell masses (values of relative mass are indicated as numbers within the graph)

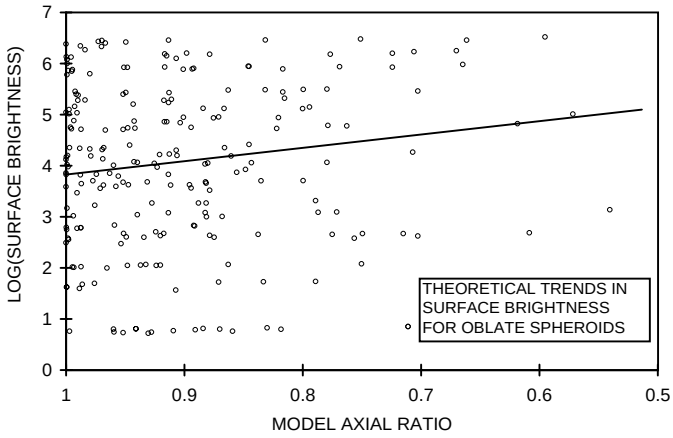

Fig. 7. Variation of surface brightness with axial ratio α for a random sample of 237 model oblate spheroids. The solid line corresponds to a least squares trend. It appears that both the scatter in results, and mean gradient $d\log(I_s)/d\alpha$ are similar to the observed trends illustrated in Fig. 9

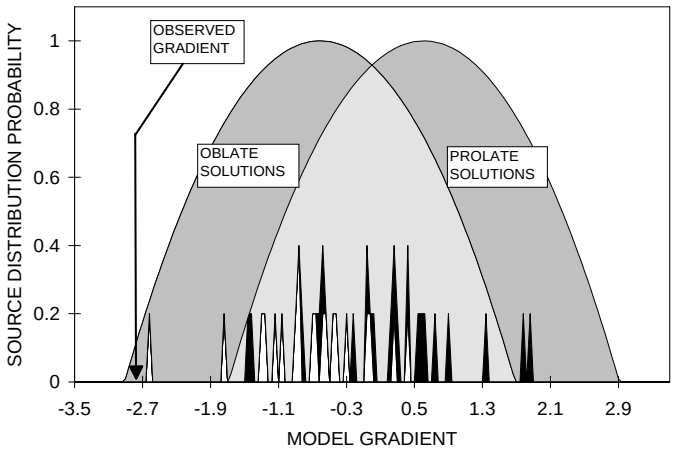

Fig. 8. Distribution of model gradients $d\log(I_s)/d\alpha$ determined using 40 Monte-Carlo simulations of surface brightness I_s against axial ratio α. Solutions relevant for prolate spheroids are indicated by the black spikes, whilst oblate solutions are represented by the white spikes. The two curves, one shifted to the right (positive model gradients) and the other to the left, correspond to the approximate ranges and distributions of deduced model gradients. Whilst prolate and oblate solutions overlap, it is clear that observed values of $d\log(I_s)/d\alpha$ are most consistent with oblate solutions

It is now pertinent to ask what trends are actually found where more detailed model simulations are undertaken. We shall assume for the purposes of this analysis that:

a) the model nebulae are oriented randomly with respect to the line of sight.
b) that the distribution of axial ratios is as illustrated in Fig. 5.
c) that the distribution of model masses is identical to that of the observed sample (i.e. as indicated in Fig. 2).
d) that the nebular filling factors ϵ are, in the mean, invariant with shell radius.

This last point needs some further explication. The proportion of the nebular volume ϵ which is filled by gas depends upon both the small scale structure of the envelopes (the clumpiness or micro-structure of the shells) and the large-scale or macro-structures of the outflows (whether the sources have large wind-blown cavities, and so forth). There have been claims that ϵ may vary with radius R (Mallik & Peimbert 1988), although it seems likely that most of these trends are due to errors in the data, and the ways in which these propagate through to the estimation of ϵ (Kingsburgh & Barlow 1992; Kingsburgh & English 1992). The best current understanding seems to be that ϵ is invariant, and we shall assume this to be the case in the proceeding analysis.

Following the rules outlined above, we have constructed a data base of 53,000 prolate and oblate model solutions, and randomly selected from these 40 subsets of 237 data points each (corresponding to the total of observed axial ratios for which there are published radio surface brightnesses (see later)). 20 of the subsets correspond to oblate structures, and 20 for prolate structures. Each of the subsets is then used to plot surface brightness against the projected (i.e. "observed") axial ratios α, and determine gradients $d\log(I_s)/d\alpha$.

An example of one such graph (derived for oblate sources) is illustrated in Fig. 7, where the gradient is $d\log(I_s)/d\alpha$ = -2.61.

The gradients thus deduced depend upon the size of the data base, and the specific (random) sample of data which is selected; variations between samples can cause wide swings in $d\log(I_s)/d\alpha$. This is illustrated in Fig. 8, where we plot individual gradients determined for the prolate and oblate model distributions (the prolate gradients are identified by shaded spikes, oblate with white spikes), and least squares solutions for the distributions of the gradients (shaded parabolas); where the shapes of the parabolas are determined from fits to the prolate and oblate solutions combined.

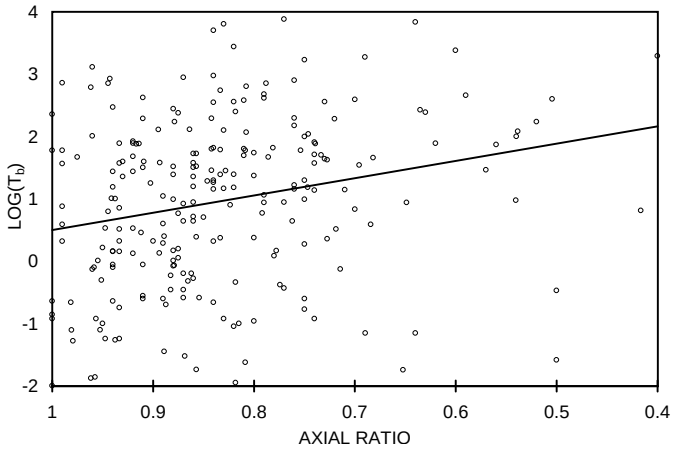

Fig. 9. Observed variation of radio surface brightness temperature T_b against axial ratio α. Although the scatter is large, this is precisely what would be expected from a Monte-Carlo analysis (see Fig. 5). The gradient is consistent with the presence of intrinsically oblate nebular structures

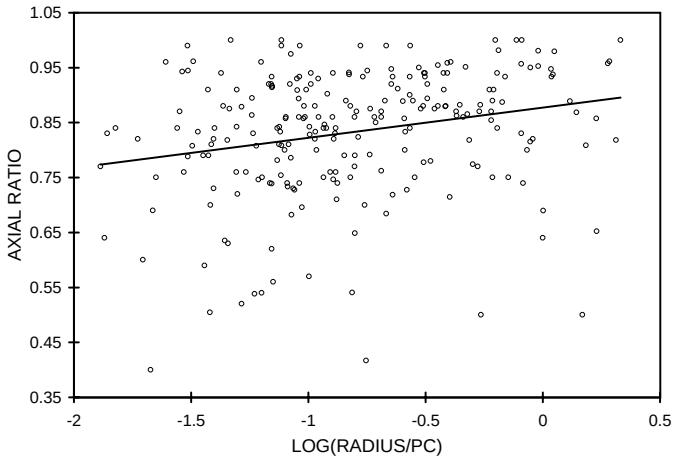

Fig. 10. Variation of observed axial ratios with values of nebular radius taken from Zhang (1995). There appears to be a trend for axial ratios to increase with increasing radius. The solid line corresponds to a linear least squares fit

It would seem, from this, that the gradients $dI_s/d\alpha$ determined for prolate models occupy a broad swathe of values to the right of the figure (i.e. towards positive values of the gradient), whilst oblate solutions are located towards negative values of gradient (i.e. to the left). It is also clear however that unlike the case of the galaxies, where both regimes were well separated, the prolate and oblate parabolas overlap - and that the overlap is appreciable. The possibilities for uncertainty are therefore rife, since oblate nebulae may give rise to gradients which are essentially indistinguishable from those for prolate sources.

It is also clear, on the other hand, that where observed gradients are large and positive (greater, say, than $d\log(I_s)/d\alpha \sim 1.8$) then observed shells would be better explained in terms of prolate solutions; with corresponding negative gradients favouring oblate solutions.

Given this situation, it is then pertinent to ask what the gradient of the observed nebular sample is - is it large and positive (i.e. consistent with oblate shells), or more consistent with trends predicted for prolate modelling?

The answer to this question may be determined from Fig. 9, where we have plotted observed axial gradients against radial surface brightnesses taken from Zhang (1995). It is clear that the scatter in the results is very similar to that deduced from our modelling; it is almost identical to that illustrated in Fig. 7. It is also clear that the gradient is $d\log(I_s)/d\alpha$ = -2.77; that is, that gradients are negative, and at the outer limits of the oblate solution range illustrated in Fig. 8.

One might therefore conclude that most nebulae are oblate, and that prolate solutions are unlikely to explain observed nebular ellipticities.

Before jumping to such a conclusion, however, it is as well to consider one further bias which has not so far been considered in this analysis. We shall note in Sect. 5 that axial ratios may increase very slightly with increasing nebular radius, with gradients $d\log(R)/d\alpha$ being of order 1.04. This is by no means an assured trend (correlation coefficients are low), but it would (if true) bias the trends in Fig. 9 towards the oblate solutions; specifically, it would of itself contribute a slope $d\log(I_s)/d\alpha \cong$ -1.96.

Deducting this component from the least-squares trend in Fig. 9 would then leave a residual gradient $(d\log(I_s)/d\alpha)_R \cong$ -0.81.

We therefore conclude that because of the unique characteristics of PN shells, it is not possible to discriminate between oblate and prolate solutions to the same degree as in elliptical galaxies. While deduced gradients $(d\log(I_s)/d\alpha)_R \cong$ -0.81 are more consistent with oblate solutions than with prolate shell structures, neither possibility can be entirely discounted.

We note, finally, that if mass loss rates (and shell masses) are greater for higher axial ratio nebulae than more circular sources, as has been proposed by Soker (2000), then this might also lead to positive gradients in the $\log(I_s)$-α plane. Such a mechanism is however little more than a theoretical speculation, and it would be interesting to see if further evidence is found to support this suggestion.

5. Evolution in ellipticities

The variation of axial ratio α against nebular radii deriving from Zhang (1995) is indicated in Fig. 10.

As may be seen, there is some evidence for an increase in mean axial ratio with increasing radius; larger nebulae are, on the whole, more circular than smaller nebulae.

We know of no modelling which has attempted to simulate such trends in detail, although such a variation is by no means implausible. Initially oblate shells might well become more circular under the continued action of radiation pressure and interior stellar winds; both of which mechanisms are expected to be spherically symmetric.

Such trends should however be treated with caution. Although it is certainly interesting to note this variation, it should

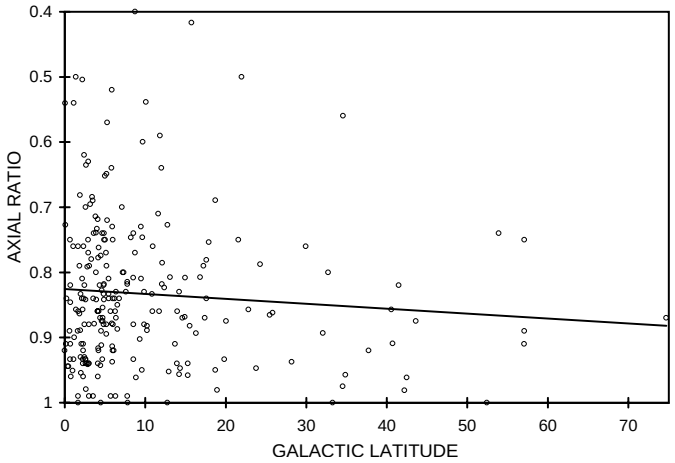

Fig. 11. Variation of axial ratio α with Galactic latitude b for all of the sources in the present sample. The least squares trend (solid line), which is marginally consistent with the hypothesis of shell deformation by the ISM, has a gradient with low statistical reliability

be pointed out that statistical determinations of radius (similar to those used here) can probably be trusted to no better than $\sim$ 40%. (Zhang 1995), whilst the correlation coefficient for the least squares fit in Fig. 8 is also small (r $\cong$ 0.24).

6. Influence of the interstellar medium and progenitor masses upon nebular ellipticities

It is by now well established that certain planetary nebulae, particularly those which are large and old, are strongly interacting with the interstellar medium (ISM). It is clear for these cases that the ram pressure of gas in the ISM, acting upon the PN envelopes, is sufficient to cause marked ellipticity of the outflows and departures from axial symmetry - as witnessed for instance by central star offsets relative to the nebular shells (e.g. Jacoby 1981; Borkowski et al. 1990; Krautter et al. 1987; Tweedy & Kwitter 1996).

Given the likely gradient of ISM density with height above the galactic plane, it then follows that such effects, where present, should increase towards the galactic plane; that nebulae with high Galactic latitudes b should be more circular that those having low values of b.

Evidence for related kinematic effects (i.e. retarded expansion velocities towards the Galactic plane) has been outlined by Hippelein & Weinberger (1990).

The present results are illustrated in Fig. 11, where it may be noted that there is indeed a slight tendency to lower axial ratios at low Galactic latitudes (note the least squares fit given by the solid line). The correlation coefficient is however low, and the significance of the trend not terribly high. A similar analysis may also be undertaken for those sources having R > 0.3 pc; sources, in brief, which are presumably more prone to such asymmetries. This however yields an almost identical outcome.

Another way of statistically expressing this conclusion is to note that mean axial ratios take the values $|\alpha|$ = 0.830 $\pm$ 0.008 where b is less than 15°, and $|\alpha|$ = 0.847 $\pm$ 0.019 for b > 15°. There is, in brief, a tendency to greater circularity at larger latitudes, although the difference is not statistically significant.

It would therefore appear that whilst shell deformation is relevant for certain nebulae, it is by no means a critical influence for the majority of PN.

A further factor which may create latitude dependent variations in α is that of progenitor mass. It is of course well known that lower mass stars will, in the main, possess larger mean galactic latitudes than stars of higher mass (see for instance Phillips 1989). It also appears that certain nebular structures depend rather strongly upon progenitor mass - the most celebrated case being perhaps that of the bipolar nebulae (e.g. Corradi & Schwarz 1995).

It is interesting, in this context, to note that Manchado, Villaver & Stanghellini et al. (2000) have claimed a dependence of nebular morphology upon galactic latitude, such that sources defined by them to have round morphologies have mean galactic latitudes |b| = 12°, whilst elliptical shells have mean latitudes |b| = 7°, and bipolars are concentrated towards |b| = 3°.

If this is so, however, and there really is a correlation between progenitor mass (and therefore latitude) and the intrinsic structures of such shells, then one must conclude that this too has left little evidence in the trends of axial ratio with latitude. It would seem that if the proportion of differing nebular types changes with b, then the mean axial ratios of these morphological types must be broadly the same.

7. Conclusions

We have determined axial ratios α for 320 circular and elliptical planetary nebulae. These data are used to analyse the distributions of intrinsic axial ratios β by assuming that the sources are prolate or oblate spheroids. We have, furthermore, evaluated theoretical trends of surface brightness with α, and compared these with observed trends, in an attempt to determine whether PN shells are oblate or prolate. Such procedures, previously employed in the study of elliptical galaxies, appear to imply that PN shells are most typically oblate in structure. We find however that various simple discriminatory tests, so useful in the case of elliptical galaxies, are significantly less clear-cut when applied to planetary nebulae. While the variation of surface brightness I_S with axial ratio α is expected to differ where shells are prolate or oblate, there is also a considerable overlap in solutions, such that gradients $d\log(I_s)/d\alpha$ may be similar for both types of shell structure. It therefore remains possible that many PN shells have intrinsically prolate configurations.

Whatever the nature of nebular structures, on the other hand, it would appear that the distribution of axial ratios is likely to be strongly peaked about β = 0.82, and to extend over a range 0.65 < β < 0.95; although an apparent deficiency of sources for β > 0.95 reflects uncertainties in the distribution of nebulae having α > 0.95. Similarly, although a certain proportion of outflows appear to possess β < 0.55, the distribution of N(β) for this regime is extremely insecure.

We note (although at a low level of confidence) that there may also be a trend for axial ratio α to increase with nebular radius R; a variation which, if true, would not be unduly surprising. There is however very little evidence for a variation of α with Galactic latitude b, suggesting that most nebulae, even those which are quite large, display little interaction with the ISM; certainly insufficient to account for observed asphericities. Similarly, it would seem (for the same reasons) that the dependence of mean axial ratio upon progenitor mass must also be quite low.

Acknowledgements. I would like to thank an anonymous referee for various useful and constructive comments. These have helped to improve the presentation of the paper.

References

Asida, S.M., Tuchman, Y. 1995, ApJ 455, 286
Atherton, P.D., Hicks, T.R., Reay, N.K., Worswick, S.P., Smith, W.H. 1978, A&A 66, 297
Balick, B. 1987, AJ 94, 671
Balick, B., Gonzalez, G., Frank, A., Jacoby, G. 1992, ApJ 392, 582
Balick, B., Preston, H.L., Icke, V. 1987, AJ 94, 1641
Basart, J.P., Daub, C.T. 1987, ApJ 317, 412
Bassgen, M., Hopfensitz, W., Zweigle, J. 1999, http://astro.uni-tuebingen.de/groups/pn/
Binney, J., & de Vaucouleurs, G. 1981, MNRAS 194, 679
Bond, H.E., Livio, M. 1990, ApJ 355, 568
Borkowski, K.J., Sarazin, C.L., Soker, N. 1990, ApJ 360, 173
Bryce, M., Balick, B., Meaburn, J. 1994, MNRAS 266, 721
Chu, Y.-H., Jacoby, G.H., Arendt, R. 1987, ApJS 64, 529
Corradi, R.L.M., Schwarz, H.E. 1995, A&A 293, 871
Curtis, H. 1918, Publ. Lick Obs. 13, 57
Dorfi, E.H., Hofner, S. 1996, A&A 313, 605
Fasano, G., Vio, R. 1991, MNRAS 249, 629
George, D., May, A. Kaftan-Kassim, Hartsuijker, P. 1974, A&A 35, 219
Greig, W., 1972, A&A 18, 70
Gurzadyan, G.A. 1970, Planetary Nebulae (Dordrecht: Reidel)
Hajian, A. 1999, aries.usno.navy.mil/ad/pne
Hajian, A.R., Frank, A., Balick, B., Terzian, Y. 1997, ApJ 477, 226
Hippelein, H., Weinberger, R. 1990, A&A 232, 129
Jacoby, G.H. 1981, ApJ 244, 903
Jewitt, D.C., Danielson, E.G., Kupferman, P.N. 1986, ApJ 302, 727
Kingsburgh, R.L., Barlow, M.J. 1992, MNRAS 257, 317
Kingsburgh, R.L., English, J. 1992, MNRAS 259, 635
Krautter, J., Klaas, U., Radons, G. 1987, A&A 181, 373
Kromov, G.S., Kohoutek, L. 1968, Bull. Astron. Inst. Czech. 19, 1
Kupferman, P.N. 1983, ApJ 266, 689
Kwok, S. 1985, AJ 90, 49
Lame, N.J., Pogge, R.W. 1994, AJ 108, 1860
Livio, M., Adam, F., Balick, B. 1996, AAS Meeting 188, #38.05
Lucy, L.B. 1974, AJ 79, 745
Manchado, A., Guerrero, M.A., Stanghellini, L., Serra-Ricart, M. 1996, The IAC Morphological Catalog of Northern Galactic Planetary Nebulae (Spain, IAC)
Mallik, D.C.V., Peimbert, M. 1988, RMA&A 16, 111
Manchado, A., Villaver, E., Stanghellini, L., Guerro, M.A. 2000, in Asymmetrical Planetary Nebulae II: From Origins to Microstructures, ASP Conference Series XXX, eds. J.H. Kastner, N. Soker & S. Rappaport
Marchant, A.B., Olsen, D.W. 1979, ApJ 230, L157
Masson, C.R. 1990, ApJ 348, 580
Merritt, D. 1992, in Morphological and Physical Classification of Galaxies, ed. G. Longo, M. Capaccioli, G. Busarello (Kluwer: Dordrecht), 309
Mihalas D., Binney J., 1981, Galactic astronomy: structure and kinematics (San Francisco: Freeman)
Pascoli, G. 1987, A&A 180, 191
Perek, L., Kohoutek, L. 1967, Catalogue of Galactic Planetary Nebulae, Academia Publishing House of the Czechoslovak Academy of Sciences, Prague
Phillips, J.P. 1989 in IAU Symp. 131, Planetary Nebulae, ed. S. Torres-Peimbert (Dordrecht: Kluwer), 425
Phillips, J.P. 1998, A&A 340, 527
Phillips, J.P. 2000, AJ (in press)
Phillips, J.P., Mampaso, A. 1988, A&A 190, 237
Phillips, J.P., Reay, N.K. 1980, ApL 21, 47
Ryden, B.S. 1992, ApJ 396, 445
Ryden, B.S. 1996, ApJ 471, 822
Sahai, R., Wootten, A., Schwarz, H.E., Clegg, R.E.S. 1991, A&A 560, 574
Sandage, A., Freeman, K.C., Stokes, N.R. 1970, ApJ 160, 831
Schwarz, H.E., Corradi, R.L.M., Melnick, J. 1992, A&AS 96, 23
Soker, N. 1992, in Proceedings of the Second ESO/CTIO Workshop (La Serena, Chile, January 21–24, 1992): Mass Loss on the AGB and Beyond, ed. H.E. Schwarz
Soker, N. 2000, in Asymmetrical Planetary Nebulae II:From Origins to Microstructures, ASP Conference Series XXX, eds. J.H. Kastner, N. Soker & S. Rappaport
Terzian, Y., Balick, B., Bignell, C. 1974, ApJ 188, 257
Tremblay, B., Merritt, D. 1995, AJ 110, 1039
Tweedy, R.W., Kwitter, K.B. 1996, ApJS 107, 255
Volk, K., Leah, D.A. 1993, AJ 106, 1954
Weedman, D.W. 1968, ApJ 153, 49
Wilson, O.C. 1958, Rev. Mod. Phys. 30, 1025
Zhang, C.Y. 1995, ApJS 98, 659
Zijlstra, A.A., Pottasch, S.R., Bignell, C. 1989, A&AS 79, 329
Zuckerman, B., Aller, L.H. 1986, ApJ 301, 772